Journal Pre-proof

Examining conductivity, current density, and sizings applied to carbon fibers during manufacture and their effect on fiber-to-matrix adhesion in epoxy polymers

Andreas Hendlmeier, Filip Stojcevski, Richard Alexander, Sunil Gupta, Luke C. Henderson

PII: S1359-8368(19)33377-3

DOI: https://doi.org/10.1016/j.compositesb.2019.107494

Reference: JCOMB 107494

To appear in: *Composites Part B*

Received Date: 15 July 2019

Revised Date: 25 September 2019

Accepted Date: 29 September 2019

Please cite this article as: Hendlmeier A, Stojcevski F, Alexander R, Gupta S, Henderson LC, Examining conductivity, current density, and sizings applied to carbon fibers during manufacture and their effect on fiber-to-matrix adhesion in epoxy polymers, *Composites Part B* (2019), doi: https://doi.org/10.1016/j.compositesb.2019.107494.

Examining conductivity, current density, and sizings applied to carbon fibers during manufacture and their effect on fiber-to-matrix adhesion in epoxy polymers.

Andreas Hendlmeier[a], *Filip Stojcevski*[a], *Richard Alexander*[b], *Sunil Gupta*[c], *Luke. C. Henderson*[a]

[a] *Carbon Nexus, Deakin University, Institute for Frontier Materials, Waurn Ponds, Victoria 3216, Australia.*
[b] *Centre for Regional and Rural Futures, Deakin University, Waurn Ponds Campus, Geelong, Victoria 3216, Australia.*
[c] *Centre for Pattern Recognition and Data Analytics, Deakin University, Waurn Ponds Campus, Geelong, Victoria 3216, Australia.*

Abstract

This study provides a comprehensive study of carbon fiber surface treatment conditions for epoxy resins. A set of 27 fibers, derived from DowAska precursor, with alterations to manufacturing conditions only occurring at the electrochemical oxidation and sizing bath. Electrolyte (NH_4HCO_3) conductivity was varied between 8, 16 and 24 µS/cm while oxidative current density was varied between 0.5, 1.0 and 1.5 A/m^2. Subsequent to oxidation, fibers were coated with either epoxy, polyamide or polyurethane compatible sizing. This study is the first to consider electrolyte conductivity, oxidative current density and sizing variables simultaneously and links them to interfacial shear strength (IFSS). Extensive chemical, physical and mechanical characterization was conducted to quantify the changes to fiber properties as a result of treatment variation. Results reveal that varying combinations of electrolyte and applied current density not only vary the degree of oxidation on the fiber, but the types of surface chemistry installed (e.g. ratio of COH, C=O, and COOH). Somewhat counter-intuitively, at high conductivities and current densities the degree of oxidized carbon species on the fiber surface is decreased. Indeed, this study shows combinations of surface treatment variables which could be used to promote the formation of surface bound functional groups in preference (e.g. phenolic groups in preference to COOH) to enhance interfacial bonding for a given resin. Determination of fiber roughness for all samples showed no statistical difference between samples, suggesting that mechanical interlocking effects do not play a role in the variations in interfacial adhesion observed herein.

1. Introduction

Carbon fiber reinforced polymer (CFRP) composites have become a staple material in modern aerospace, automotive, and civil engineering industries. Despite the benefits gained in both light weight and high strength performance, CFRP composites have an inherent flaw relating to premature failure through interfacial debonding [1-4]. The cause of interfacial debonding is poor physical and chemical compatibility between fibers and matrix at the bonding junction known as the interface [5-7].

As such, the current performance of composite materials remains at approximately 10% of the theoretical maximum achievable [8]. Thus, research addressing interfacial debonding failures in a manner that can be immediately employed on existing carbon fiber manufacturing lines is of great merit to the composites industry as a whole. Carbon fiber manufacturers currently use two methods of surface treatment during fiber manufacturing to improve fiber-to-matrix bonding. These are electrochemical oxidation and sizing.

Electrochemical oxidation is the process of passing fibers through an electrolyte solution and applying a potential to the fibers, generating a current density, in turn alters fiber topography [9-14], and attaches non-native moieties to the fiber surface which are more compatible with matrix bonding [15-25]. Sizing is the process of applying a thin polymer film to the outside of the fibers subsequent to oxidation. Conflicting literature both supporting [26-30] and refuting [19,31-33] sizings role as a means of improved interfacial adhesion exists, highlighting a discontinuity in understanding. Undoubtedly,

sizing is a necessary step in fiber fabrication as it protects fiber bundles from damage during the weaving process [34-37] and binds them together which is required to convert spooled fiber into fabric or preform used to make composite parts [38,39].

While both electrochemical oxidation and sizing have shown cases of improved interfacial adhesion, the root cause for why fiber-to-matrix bonding improves remains disputed. Where some research suggest mechanical interlocking caused by modified topography is the primary mechanism for improved interfacial adhesion [40], other research suggest mechanical interlocking plays no direct role on performance [26,41]. Where some research suggests the introduction of oxygenated functional groups to the fiber surface are the primary mechanism for improved adhesion [16,20,42], others suggest non-native functional groups play a detrimental role [43] or no role at all [19]. While simultaneously a growing majority is arguing that interfacial adhesion is compatibility issue between fiber-interface-matrix which must be considered on a case by case basis [4,44-46].

Regardless of the perspective taken, an area of conflicting understanding clearly exists which must be clarified to further composite performance and fiber manufacturing quality.

This can only be achieved by addressing the causes of why literature remains conflicted. A lack of uniformity in precursor selection, fiber choice, manufacturing parameters and the ambiguity of sizing chemistry have created a body of knowledge that may not necessarily be comparable. Specifically research considering multiple surface treatment variables simultaneously is scarce which contributes to current confusion. As one input variable on a manufacturing line changes so do all others. No research has ever considered the combination of electrolyte conductivity, amperage and sizing simultaneously.

Research conducted by Gulyas *et al.* [42] considered the effects of electrochemical oxidation and highlights the sensitivities of changing multiple input parameters. A selection of electrolytes were considered with voltage and electrolyte concentration varied. Using a NaOH electrolyte, when bath concentration was maintained at 20 wt% and voltage increased, IFSS linearly decreased. When voltage was maintained at 5 V and electrolyte concentration raised, IFSS linearly increased. When the same conditions were applied in a Na_2SO_4 electrolyte, the opposite trends were observed. To further confuse this relationship, when the same conditions were applied in a HNO_3 electrolyte, trends changed dependent on each voltage condition alone, on a case-by-case basis. Modifying one input parameter simultaneously effects the control of others. It is worth noting this study provided no investigation of the subsequent role of sizing.

In a similar study conducted by Gnädinger *et al.* [45] the variability of sizing chemistry of fibers in epoxy resin was explored by comparing epoxy, polyurethane, polyamide sized and unsized fiber. While trends showed sizings to improve adhesion, this was only true if fibers had been previously been oxidized. No consideration into the oxidation parameters was considered, and as such, the study was unable to effectively explore the link between both oxidation and sizing concurrently.

Inspired by previous studies and the existing academic confusion, this publication aims to bridge the gap in understanding the concurrent effects of oxidation and sizing together. It is worth noting that in previous multivariate studies mentioned [42], fibers used non-industry scale precursors. By using a DowAksa precursor which accounts for up to 36,000 metric tonnes per year of the current carbon fiber global supply chain [47], ammonium bicarbonate electrolyte which is the standard electrolyte for carbon fiber manufacturing [48-50]. Michelman sizings [51,52] a prominent supplier of sizings worldwide, and epoxy resin, which remains the largest market for CFRP composites, this study, aims to provide the widest impact to immediate composite research possible.

In this study electrochemical conductivity, current density, and sizing are varied to provide a subset of 27 carbon fibers which were characterized topologically, chemically, and physically. Interfacial adhesion was subsequently assessed to form associate treatment variables and bonding performance. Results are also complimented by a mathematically derived model for interfacial adhesion which aims predict interfacial adhesion dependent on surface treatment parameters. This is only a preliminary attempt at modelling which we hope is taken up by others and, to the author's knowledge, has only been attempted once before [53]. As such, it is hoped this paper becomes a staple for interested readers considering how carbon fiber surface treatments effect mechanical adhesion and how they may be optimized to address debonding.

2. Materials & Method

2.1 Raw Materials

Carbon fibers were created at the Carbon Nexus research facility [54] using DowAska precursor. The stabilization and carbonization temperatures, draw lengths and tension have been kept confidential as required by the supplier. Subsequent to carbonization, fibers were passed through an electrochemical oxidative bath and a sizing bath. The electrolyte used during oxidation was ammonium bicarbonate and the conductivity of the solution and the potential applied to the fibers was varied between 8, 16 and 24 µS/cm and 0.5, 1 and 1.5 A/m^2, respectively. Subsequent to oxidation fibers were washed and dried before being placed through a sizing bath. The sizings used were epoxy (Hydrosize EP834S), polyamide (Hydrosize PA845H) and polyurethane (U480). By varying all three variables a collection of 27 fibers were created. To assist readers, a coding system was created to name fibers as denoted in Table 1.

Table 1: Classification code for fibers used within this paper grouped by sizing, current density and conductivity.

Epoxy Sized Fibers			Polyamide Sized Fibers			Polyurethane Sized Fibers		
Sample	Current density	Conductivity	Sample	Current density	Conductivity	Sample	Current density	Conductivity
EP1	Low	Low	**PA1**	Low	Low	**PU1**	Low	Low
EP2	Medium	Low	**PA2**	Medium	Low	**PU2**	Medium	Low
EP3	High	Low	**PA3**	High	Low	**PU3**	High	Low
EP4	Low	Medium	**PA4**	Low	Medium	**PU4**	Low	Medium
EP5	Medium	Medium	**PA5**	Medium	Medium	**PU5**	Medium	Medium
EP6	High	Medium	**PA6**	High	Medium	**PU6**	High	Medium
EP7	Low	High	**PA7**	Low	High	**PU7**	Low	High
EP8	Medium	High	**PA8**	Medium	High	**PU8**	Medium	High
EP9	High	High	**PA9**	High	High	**PU9**	High	High

The resin used in testing was Bisphenol A derived, RIMR 935 epoxy mixed with RIMH 936 amine hardener mixed at a parts by weight ratio of 100:29, respectively. Epoxy was thoroughly mixed for 15 minutes before being placed under a -100 kPa vacuum to remove any latent microbubbles. Resin was then used in sample production (*section 2.3* Single Fiber Fragment Testing (SFFT)).

2.2 Characterization

2.2.1 Fiber Tensile Testing

Single fiber tensile strength, fiber modulus and linear density of all configurations were determined using a Favimat single fiber tester (Textechno H. Stein, Germany). Individual fibers were carefully extracted from pristine tows using wax tipped tweezers and cut to a length of approximately 5 mm. A

0.8 gram pre-weight was attached to one end of the fiber before being loaded into the Favimat robot. 75 fibers of each fiber configuration were tested at a loading rate of 2 mm/min in accordance to ASTM D1577.

A two-parameter Weibull probability distribution (P) was performed for all fiber types. This function provides the cumulative probability of the fibers to undergo premature failure with a linear distribution of data points denoting confidence that fiber variability in each configuration is negligible. Weibull probability 'P' is determined using Equation 1 where σ is the applied tensile strength, m is the Weibull shape parameter, and σ_0 is the characteristic fiber stress. All values determined via Weibull analysis (m and σ) can be found in the accompanying ESI.

$$P = 1 - \exp\left[-\left(\frac{\sigma}{\sigma_0}\right)^m\right]$$

Equation 1

2.2.2 XPS

XPS analysis was performed using an AXIS Ultra-DLD spectrometer (Kratos Analytical Inc., Manchester, UK) with a monochromated Al Kα source (hv = 1486.6 eV) at a power of 150 W (15 kV × 10 mA), a hemispherical analyzer operating in the fixed analyzer transmission mode and the standard aperture (analysis area: 0.3 mm × 0.7 mm). The total pressure in the main vacuum chamber during analysis was typically below 10^{-8} mbar. The fiber samples examined for XPS were taken from the manufacturing line before exposure to the sizing bath, thus providing an idea of the underlying surface chemistry of each treatment.

Bundles of fibers were suspended across a custom-designed frame attached to standard sample bars. This ensured that only the sample to be analyzed was exposed to the X-ray beam and that any signal other than that originating from carbon fibers was excluded. Each specimen was analyzed at a photoelectron emission angle of 0° as measured from the surface normal (corresponding to a take-off angle of 90° as measured from the sample surface). However, since the microscopic emission angle is ill-defined for fibers the XPS analysis depth may vary between 0 nm and approx. 10 nm (maximum sampling depth).

Data processing was performed using CasaXPS processing software version 2.3.15 (Casa Software Ltd., Teignmouth, UK). All elements present were identified from survey spectra (acquired at a pass energy of 160 eV). To obtain more detailed information about chemical structure, C 1s, O 1s and N 1s high resolution spectra were recorded at 20 eV pass energy (yielding a typical peak width for polymers of 1.0 eV). If required these data were quantified using a Simplex algorithm in order to calculate optimized curve-fits and thus to determine the contributions from specific functional groups. The atomic concentrations of the detected elements were calculated using integral peak intensities and the sensitivity factors supplied by the manufacturer. Atomic concentrations are given relative to the total concentration of carbon as follows: the concentration of a given element X was divided by the total concentration of carbon and is presented here as the atom number ratio (or atomic ratio) X/C. This value is more robust than concentrations when comparing different samples. Binding energies were referenced to the aliphatic hydrocarbon peak at 285.0 eV. The accuracy associated with quantitative XPS is ca. 10%-15%. Precision (i.e. reproducibility) depends on the signal/noise ratio, but is usually much better than 5%. The latter is relevant when comparing similar samples.

2.2.3 AFM

Surface topography and roughness of unsized fibers was determined using atomic force microscopy (AFM). A Bruker Dimension SPM 3000 was used at a scan rate of 0.5 µm/min. A silicon nitride pyramid probe with a spring constant of 0.12 N/m was used for contact mode mapping. Single fibers were

mounted on glass microscope slides with 27 individual taken at a 1x1 µm scale. Images were then processed using NanoScope Analysis 1.4 software in which a second order flattening was applied to remove fiber curvature. Roughness was calculated using arithmetic roughness average (R_a) (Equation 2) where z(x) is the depth function of peaks and troughs across the fiber surface and L is the length of image.

$$R_a = \frac{1}{L}\int_0^L |Z(x)|dx$$

Equation 2

2.3 Single Fiber Fragment Testing (SFFT)

Single fiber fragmentation test (SFFT) samples were created by carefully extracting single fibers of approximately 12 cm length from pristine tow bundles. Sticky tape was then adhered to and folded at either end of the individually extracted fibers and mini wooden pegs attached to said tape. Fiber filaments were then positioned into a specially designed silicon mould (see ESI) and pre-tensioned to 3.4 mN by the weight of the wooden pegs. A 3 mL syringe was used to inject resin into the dog-bone mould ingress which completely submerged the fibers. Resin was then allowed to cure for 48 hours at room temperature before being post cured at 100 °C for 12 hours. Samples were then de-moulded placed under tensile testing.

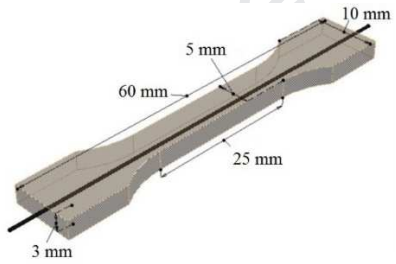

Figure 1: Single fiber fragmentation testing (SFFT) coupon dimensions used in this study.

Tensile testing was conducted by the securing dog-bone samples (Figure 1) into a 10 kN Instron tester (Instron Pty Ltd, USA). Mechanical jaw clamps were used to secure the samples into position. Samples were elongated at a rate of 0.05 mm/min until an elongation of 2 mm was reached in accordance to the respective Riso protocol [55].

By loading the samples in this manner the difference in elongation properties between the fibers and resin causes fragments to occur at the carbon fiber-matrix interface. As stress across the interface increases and surpasses fiber tensile strength (determined prior via Favimat testing), fiber begin to fragment. The length at which fibers can no longer break due to stresses at the interface being insufficient to cause failure is called the critical crack length (l_c). Dependent on the bonding strength at the interface fibers will fragment at different sizes. Smaller fiber lengths denote better bonded interface as a greater load is transferred across a smaller area.

Subsequent to tensile loading an Olympus DP70 polarized microscope was used to measure the fiber fragment lengths of each sample. The critical crack length of each fiber configuration was calculated using Equation 3. Similarly the IFSS of each fiber configuration was determined using Equation 4 where fiber diameter (d) and fiber tensile strength (σ_f) were determined prior via Favimat testing.

$$l_c = \frac{4}{3}\bar{l}$$

Equation 3

$$\tau = \frac{\sigma_f d}{2 l_c}$$

Equation 4

2.4 Statistical Analysis

All comparisons presented in this work were analyzed using a two-tailed T-Test with equal variance. Statistical significance was taken to be any data comparison in which a P-value of less than 0.05 was obtained.

3. Results

3.1 Fiber Mechanical Properties

The break tension and elastic modulus of all fibers created are of automotive grade. For comparison Toray T300 fibers have a tensile modulus of 230 GPa and a break tension of 3.5 GPa. Table 2 shows the tensile modulus values of all fibers dependent on the sizing and grouped by the treatment classification code outlined in Table 1.

Table 2: Tensile modulus (GPa) of all fiber types grouped by treatment conditions and colored by sizing type.

		Epoxy Sized			Polyamide Sized			Polyurethane Sized		
Conductivity		Low	Medium	High	Low	Medium	High	Low	Medium	High
Current density	Low	249.2±39.2	234.1±20.6	230.9±14.4	252.8±32.7	249.1±6.5	242.6±6.9	230.1±10.9	234.0±7.9	233.1±11.6
	Medium	228.7±15.7	239.9±17.1	238.9±17.2	246.5±8.4	243.9±6.9	247.1± 7.5	236.0± 6.3	230.5±13.2	239.6±6.1
	High	232.3±19.4	237.7±16.5	234.4±10.9	241.5±10.4	240.2±33.65	250.9±8.5	231. 3± 10.2	231.7±21.6	238.5±7.9

All fiber types had a tensile modulus greater than 230 GPa. For configurations 1 (8 µS/cm @ 0.5 A/m^2) and 6 (16 µS/cm @ 1.5 A/m^2), polyurethane fibers were found to be statistically different to both the epoxy and polyamide sized fibers, while the latter two fibers were statistically indistinguishable. For configurations 3 (8 µS/cm @ 1.5 A/m^2), 4 (8 µS/cm @ 1.5 A/m^2) and 8 (24 µS/cm @ 1 A/m^2) polyamide sized fibers were statistically different to the other, while the remaining two were both statistically similar. For all other configurations, fibers with different are statistically different to one another ($P < 0.05$). Complete data for statistical comparisons is available in the accompanying ESI.

Table 3: Break tension (GPa) of all fiber types grouped by treatment conditions and colored by sizing type.

		Epoxy Sized			Polyamide Sized			Polyurethane Sized		
Conductivity		Low	Medium	High	Low	Medium	High	Low	Medium	High
Current density	Low	3.4± 0.79	2.94±0.53	3.07±0.73	3.39±0.41	3.38±0.43	3.38±0.47	3.09± 0.85	3.25±0.59	3.28±0.53
	Medium	2.91±0.81	3.42±0.47	3.19±0.49	3.52±0.44	3.59±0.46	3.58±0.43	3.26±0.46	3.07±0.50	3.71±0.45
	High	3.10± 0.85	3.29±0.54	3.16±0.52	3.46±0.47	3.34±0.66	3.43±0.64	3.17± 0.74	3.19±0.75	3.28±0.44

The effects of altered mechanical performance are not being attributed to any changes to the carbon fiber microstructure which is the governing factor of modulus [56,57]. However as seen by the slightly increased modulus for all polyamine fibers, the addition of a sizing polymer may have an effect which alters stress-strain response. Regardless of fiber selection, all fibers created were within a comparable margin to automotive grade.

The ultimate break tension (Table 3) of all carbon fibers within this study grouped by sizing type and the by treatment classifications outlined in Table 1. Configuration 1 (8 µS/cm @ 0.5 A/m^2) was the only case which polyamide and polyurethane sized fibers were statistically different from one another while epoxy sized fibers remained statistically indistinguishable to both fiber types. Conversely, configuration 3 (8 µS/cm @ 1.5 A/m^2) found polyamine fibers to be different to all others while epoxy and polyurethane were in-line with one another. Configuration 6 (16 µS/cm @ 1.5 A/m^2) showed all fibers to be homogenous to one another while all other configurations showed statistical difference across the three fiber types for the same treatments (ESI).

While the variance between fibers is statistically different when considering such a large data set, it is worth nothing that break tension for all fibers is within ±0.6 GPa. As break tension is largely governed by fiber flaws [11,58,59], it is possible that damage may have been induced during extraction of single fibers from pristine tows as well as spooling damage which is likely the attributing cause of statistical variance.

3.2 Interfacial Shear Strength (IFSS) and surface chemistry.

Discussion of XPS for all treated fibers

Analysis of the low conductivity (8 µS/cm) (Figure 4, left) shows that the total amount of oxidized carbon species increases rapidly with increasing current density. This observation is consistent with the decreasing graphitic nature of the carbon fibers, as the current density is increased, correlating the conversion of sp^2 hybridized carbons to sp^3 via the introduction of oxidation products (table provided in ESI). Interestingly, the major portion of these oxidation products seems to be derived from the presence of phenolic (C-OH) and carboxylate (COOH) functionalities, while the signal attributed to the ketone moiety remains consistent over the applied current density range. Comparing this to the sample with moderate conductivity (12 µS/cm, Figure 4, middle), has the opposing trend whereby the total amount of oxidized carbon species is highest for low applied current density and then rapidly drops (and plateaus) for the medium and high current density samples. The majority of this additional oxidized carbon species is apparently derived from the carboxylate species present on the fiber surface, as this is very high at low current density and similarly, is drastically reduced as increasing current density is applied. These data suggest that the interplay between electrolyte concentration and applied current density to the fibers during surface treatment may effect different changes in the fibers on the molecular scale and thus lead to variable preference for sizings and resins

Similarly, examination of the XPS data for fibers surface treated at high conductivity (16 µS/cm, Figure 4, right) showed similar oxidized carbon trend as the previous example whereby a decrease in total oxidized carbon species at increasing current density. However, in this example, no plateau is observed and a sharp successive decrease is observed from low to medium to high. Unlike the previous example the majority of the oxidized carbon in the low current density sample in this case seems to be derived from phenolic and alcoholic units being introduced. This again suggests that the combination of applied current density and electrolyte may cause variable manifestations of surface chemistry. The decrease of total oxidized carbon in these latter examples at medium/high current density may be due to the rapid oxidation and exfoliation of carbon nanoplatelets from the carbon fiber surface. This process has been observed previously using highly oxidative techniques and thus the surface observed by XPS may just be freshly revealed graphitic carbon.

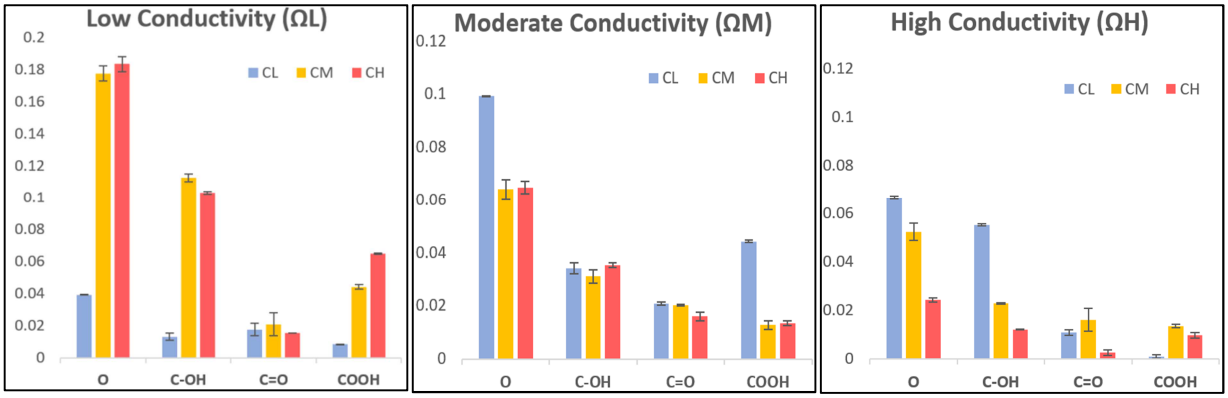

Figure 2: Deconvoluted high-resolution C1s spectra (of fibers prior to sizing) broken down into total amount of oxidized carbon (Total, designated as 'O'); alcoholic (C-OH), carbonyl (C=O), and carboxylic acid (COOH) signal contributions.

Interfacial shear strength (IFSS) of treated fibers with epoxy-sizing.

Examination of the IFSS for Michelman Hydrosize EP834S sized fiber (epoxy compatible) in an epoxy resin showed high values across most of the treatment combinations. With respect to the low conductivity samples showed statistically indistinguishable IFSS values, despite the low current density sample showing a greatly reduced amount of oxidized carbon species, relative to the medium and high current density treated fibers. This is in direct contrast to literature suggesting that increasing surface oxidation is correlated to an increase in IFSS [15,21,42,60-63]. When the same current densities were applied to carbon fibers in a moderate concentration of electrolyte the opposite trend is seen whereby the lowest current density applied during surface treatment resulted in the highest amount of oxidized carbonaceous species for all three samples, the majority of which arose from additional carboxylic acid groups. Again, the commonly held assumption that surface polarity corresponds to increases in IFSS was not consistent with the values obtained here with the low and medium current density treated fibers showing indistinguishable IFSS values (Figure 5). Similarly, the medium and high current density treated fibers, which possessed almost identical amounts (and constituents) of oxidized carbon groups, showed a statistically significant reduction in IFSS for the latter sample. Finally, treating the fibers in a highly conductive environment led to yet another trend with respect to total oxidation whereby a consistent decrease in oxidized species was observed with increasing applied current density. In this instance the fibers treated with the medium current density outperformed those treated with low and high current densities, with respect to IFSS. Considering the nature of an epoxy polymer, the presence of ring-opened epoxide groups will result in a substantial amount of alkyl alcoholic groups, able to extensively hydrogen bond. The degree of oxidation generally correlated with higher IFSS but of these oxidized species the carbonyl-derived (C=O) appeared to have minimal impact on IFSS. This is consistent with the hydrogen bonding capability of these functional groups as carbonyl species (ketones, aldehydes, esters, etc.) can only participate in this interaction by receiving hydrogen bonds while alcohols (C-OH) and carboxylic acids (COOH) can participate by both giving and receiving hydrogen bonds. This effect may lead to better sizing-surface-resin interactions and therefore manifest as improved IFSS.

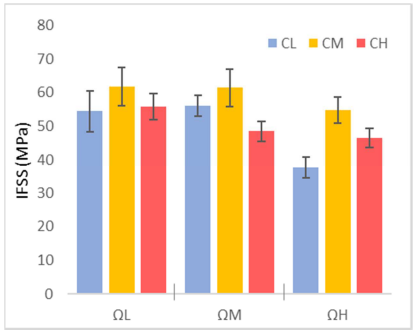

Figure 5: IFSS values as determined by single filament fragmentation for each epoxy sized-fiber sample, CL = Conductivity: Low; CM = Conductivity: Medium; CH Conductivity: High.

Interfacial shear strength (IFSS) of treated fibers with polyamide-sizing.

In this instance, the fibers were sized with a polyamide-derived material (Michelman Hydrosize PA845H), which is not optimal for epoxy, generally due to the thermoplastic vs. thermoset nature of each polyamide and epoxy, respectively. The intention here was to see if, despite the use of a non-compatible sizing, if any variation in surface chemistry affected the IFSS or if these changes were masked by the sizing. Unsurprisingly, the observed IFSS values were reduced, relative to the epoxy-sized fibers, but nevertheless large variations in IFSS were still observed suggesting that the surface chemistry still plays an important role in these instances. The most promising results were observed for the sample treated with both medium and high current density at a moderate conductivity. Interestingly, these treatment conditions correlated to a significant reduction in the carboxylic acid component of the surface, suggesting that the high polarity of those functional groups is not conducive to favorable sizing-surface interactions. This makes sense with the underlying chemistry of a generic polyamide polymer, as these are largely lipophilic (e.g. Nylon-6,6) interspersed with small amide moieties capable of weak hydrogen bonding [64]. Therefore, the presence of phenols and ketone/carbonyl derived functional groups would provide the opportunity for hydrogen bonding while not providing the surface with extreme (and incompatible) polarity of a COOH group.

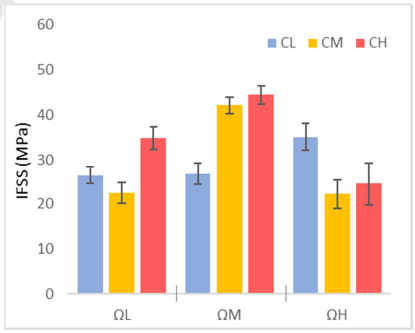

Figure 6: IFSS values as determined by single filament fragmentation for each polamide-sized fiber sample, CL = Current density: Low; CM = Current density: Medium; CH = Current density: High.

Interfacial shear strength (IFSS) of treated fibers with polyurethane-sizing.

Finally, polyurethane (PU) sized fibers were also assessed as a 'middle ground' between epoxy and polyamide sizings. On the whole, again, the fibers treated with at a medium conductivity at all current densities were the optimal from an IFSS perspective. The only outlier in this instance is the fibers treated at low conductivity and high current density, which showed excellent IFSS, though there is nothing remarkably different, with respect to surface chemistry, between this sample and the one treated at a medium current density. By far, the worst performing samples were those treated with variable current densities at high conductivity, where all observed IFSS values were statistically

indistinguishable. Examining the samples treated with a low conductivity there is a significant increase in IFSS when a high current density is used. Correlating this to the surface chemistry (Figure 4) shows very similar proportion of oxidized carbon species for the medium and high current density treatments. The only notable difference between these samples is the relative amount of C-OH:COOH functional groups, with the former (medium current density) being slightly higher in C-OH than COOH, while for the latter (high current density) this relative amount is reversed. This subtle difference manifesting as a significant difference in IFSS is puzzling, though the most consistent IFSS values were observed for the fibers treated at medium conductivity and current density. The surface chemistry of these fibers show a moderate amount of all alcohol (C-OH), carbonyl (C=O), and carboxylic acid (COOH) groups suggesting that this interaction may be a balance of all these interactions rather than just dominated by one.

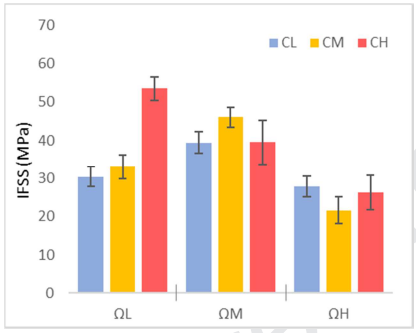

Figure 7: IFSS values as determined by single filament fragmentation for each polyurethane-sized fiber sample, CL = Current density: Low; CM = Current density: Medium; CH = Current density: High.

While there is no clear and quantifiable trend within these data, they do highlight that there is a critical interplay between oxidation conditions (current density/potential) and the amount of electrolyte present in solution. Also, the relative ratio of these two variable can considerably change not only the amount of surface oxidation which is achieved, but the types of functional groups installed can be substantially different. This may be due to the nature of electrical double layer formed at the fiber surface in each of these conditions, the accessibility of water to the fiber surface to induce oxidation, or the relative etching rates of graphene/graphite from the surface of the fibers at each conductivity. Indeed, the approach of introducing high levels of surface functional groups via the application of high current densities and high conductivities is not true, indeed it is the opposite given these results.

3.3 Topological Characterization

The surface roughness of all fiber considered in this study was determined using AFM and is provided (Table 4

Current density	Conductivity	Epoxy	Polyamide	Polyurethane	Unsized
Low		38 [14]	31 [12]	34 [15]	-
Medium	**Low**	29 [10]	31 [14]	29 [12]	-
High		28 [12]	27 [10]	29 [9]	-
Low		32 [12]	28 [10]	30 [9]	-
Medium	**Medium**	31 [12]	30 [12]	39 [12]	-
High		32 [15]	32 [11]	32 [11]	-
Low		22 [10]	28 [12]	32 [10]	-
Medium	**High**	26 [9]	28 [11]	34 [13]	-
High		31 [12]	30 [13]	32 [15]	-
No treatment		-	-	-	22 [6]

). Authors would note, that due to the large error bars observed in data, no trends can be discussed with certainty, though in general the roughness of the fibers was very low. Consequently, a definitive discussion of roughness as a function of surface treatment conditions and sizings may be misleading. For the interested reader a discussion of the average roughness of fibers and their relation to IFSS has been provided in the accompanying ESI.

Table 4: Roughness of each fiber type, Ra, in nm including standard deviation in brackets

Current density	Conductivity	Epoxy	Polyamide	Polyurethane	Unsized
Low		38 [14]	31 [12]	34 [15]	-
Medium	**Low**	29 [10]	31 [14]	29 [12]	-
High		28 [12]	27 [10]	29 [9]	-
Low		32 [12]	28 [10]	30 [9]	-
Medium	**Medium**	31 [12]	30 [12]	39 [12]	-
High		32 [15]	32 [11]	32 [11]	-
Low		22 [10]	28 [12]	32 [10]	-
Medium	**High**	26 [9]	28 [11]	34 [13]	-
High		31 [12]	30 [13]	32 [15]	-
No treatment		-	-	-	22 [6]

Consistent with the observed roughness, no correlation between increases in surface roughness and improved IFSS was observed. This suggests that mechanical interlocking is not the primary mechanism for variations in fiber-matrix bonding in this study and surface roughness played little to no direct role in interfacial performance. This is in-line with some existing literature [26,41]. However, the secondary effects of topological modification such as the exfoliation of weak graphitic layers from the fiber surface to expose active carbon sites cannot be ruled out as an important factor in fiber-to-matrix bonding.

4. Mathematical interaction of variables and their effect on IFSS.

Using the IFSS data and treatment variables, three mathematical models were created to investigate the interaction of each variable. It is important to note that the following model uses a very small pool of data and thus we do not recommend its use to predict IFSS. Our intention here is to show that, even from a small volume of data, the variables used in this study and their interaction is very complex and typically non-linear. We hope that as our research effort (and others efforts) continues, that this pool of data will be added to and a more comprehensive model from which reliable trends and correlations can be observed. Here we present our first effort in this area, and complements recent work by Kamps *et al.* [53]. Each model was grouped by respective sizing compound. A linear least squares method was applied with a second order non-linear component included to account for sensitivity to treatment (Equation 5). Extrapolation of n = 9 data points per model was used to create Equation 6 where y = interfacial shear strength (MPa), x_1 = applied current density (A/m^2) and x_2 = solution conductivity (µS/cm). Coefficients c_0, c_1 and c_2 consider the linear effects of current density, conductivity and sizing directly on IFSS performance. Coefficient c_3 is the coupling constant that denotes the impact current density and conductivity have on one another when a change in either or both occurs. While coefficients c_4 and c_5 applied to second order terms represent the non-linear sensitivities of the mathematical model to changes in current density and conductivity respectively. The coefficients required to complete Equation 6 for each sizing model are listed in Table 5. In the scenario that either x_1 or $x_2 = 0$ only the linear portion of the equation is relevant. For all other cases, coefficients c_3, c_4 and c_5 must be applied.

By considering c_1 and c_2 we observe current density to be the dominating factor to IFSS performance for epoxy sized fibers with conductivity playing a near negligible role to IFSS. Conversely conductivity

was the governing factor to IFSS performance for polyamide sized fibers, while polyurethane sizing showed responsiveness to both current density and conductivity change.

$$\min_{c_0,c_1\ldots c_5} \sum_{i=1}^{n} [y_i - (c_0 + c_1x_1 + c_2x_2 + c_3x_1x_2 + c_4x_1^2 + c_5x_2^2)]^2$$

Equation 5

$$y = c_0 + c_1x_1 + c_2x_2 + c_3x_1x_2 + c_4x_1^2 + c_5x_2^2$$

Equation 6

Table 5: Coefficient values for mathematical model to predict IFSS, Equation 7. (P values from t-tests)

Coefficient	Detail	Epoxy	Polyamide	Polyurethane
c_0	Intercept	27.22 (0.24)	-16.67 (0.65)	-7.45 (0.80)
c_1	Current density	69 (0.09)	0.33 (0.99)	14.67 (0.73)
c_2	Conductivity	0.56 (0.77)	6.19 (0.13)	5.40 (0.11)
c_3	Coupling term	0.44 (0.50)	-1.19 (0.32)	-1.56 (0.14)
c_4	Second order non-linear sensitivities	-37.33 (0.06)	12 (0.63)	8.67 (0.67)
c_5		-0.05 (0.37)	-0.16 (0.18)	-0.15 (0.13)

Similarly, polyurethane sized fibers have the largest coupling coefficient (c_3) indicating that changes to either input variable will have a notable impact to the effects of the secondary treatment condition across the three sizings. In all cases the c_4 sensitivity coefficient shows the current density plays a much greater impact on IFSS non-linearity than conductivity. Hence alterations to current density are more likely to alter predictability of the model than changes conductivity.

The average error of the epoxy, polyamide and polyurethane models was 2.69 MPa, 2.27 MPa and 4.83 MPa which correlated to an average percentage error of 6.50%, 6.91% and 10.76%, respectively. Representative figures showing the models plotted against experimental data points is available in the accompanying ESI. While these models may not be perfect, they are one of the first attempts to create a governing equation to predict IFSS performance with respect multiple treatment variables while also highlighting which treatments are driving adhesion. It is hoped that this approach will set a precedence for future researchers considering a multivariate analysis of fiber treatment.

5. Conclusion

In conclusion, we have fabricated 27 novel carbon fibers which were the result of varying surface treatment conditions, specifically the conductivity of the surface treatment bath amperage applied to the fibers (9 samples). Each of these samples was then sized with a commercial sizing which was based on a different resin type (epoxy, polyamide, and polyurethane) giving a comprehensive cross section of carbon fibers. Characterization of these fibers showed that they were consistent with automotive grade materials and the alteration of these manufacturing variables had minimal effect on ultimate fiber properties. Examination of the surface chemistry via XPS showed that the specific combination of current density and conductivity applied to the fibers manifests as vastly different surface chemistry, with higher applied current density often resulting in lower carboxylic acid content, and more phenolic/alcoholic groups. Conversely, the fiber surface roughness was measured for each sample and

the difference between samples was found to be negligible. Determination of interfacial shear strength showed that fibers treated with high current densities (1.5 A/m^2) and high conductivity (24 µS/cm) were typically the worst performing in epoxy resin, regardless of sizing. Whereas, in general, fibers which were treated at medium current densities (1 A/m^2) and medium conductivity (16 µS/cm) were the best performing across all sizings. The absence of a clear correlation between processing parameters, IFSS, and sizing combinations suggests that there exists a dynamic and unpredictable relationship between these variables. All variables and determined IFSS values were mathematically modelled using the generated data and it was found that non-linear interactions were present for each set of sizings. Additionally, the modelling showed that the application and variation of current density to the fibers would result in the largest changes to IFSS. While this may seem obvious, our findings regarding the variability of surface chemistry installed using different conductivities would suggest that a 'less is more' approach is often the best way to achieve a high IFSS. Extensions of this study using a larger data set are currently underway, to increase the certainty of our mathematical model, and will be reported in due course.

6. Acknowledgements

This work was funded by the Australian Research Council via the ARC Training Centre for Lightweight Automotive Structures (IC160100032), The ARC Future Fiber Hub (IH140100018), and the ARC Discovery Program (DP140100165, DP18010094). We would like to acknowledge the Carbon Nexus team for manufacturing the fibers. We would also like to acknowledge the help of Dr. Thomas Gengenbach (CSIRO Manufacturing, Clayton, Victoria, Australia) in performing XPS analysis of fiber samples. We also thank Ford USA for their contribution and support. This work was performed in part at the Deakin node of the Australian National Fabrication Facility, a company established under the National Collaborative Research Infrastructure Strategy to provide nano and micro-fabrication facilities for Australia's researchers.

7. References

1. Graciani, E.; Mantič, V.; París, F.; Varna, J. Fiber–matrix debonding in composite materials. In *Modeling Damage, Fatigue and Failure of Composite Materials*, Talreja, R., Varna, J., Eds. Woodhead Publishing: 2016; https://doi.org/10.1016/B978-1-78242-286-0.00007-8pp. 117-141.
2. Drzal, L.T.; Madhukar, M. Fiber-matrix adhesion and its relationship to composite mechanical properties. *Journal of Materials Science* **1993**, *28*, 569-610, doi:10.1007/bf01151234.
3. Jones, C. The chemistry of carbon fiber surfaces and its effect on interfacial phenomena in fiber/epoxy composites. *Compos. Sci. Technol.* **1991**, *42*, 275-298, doi:https://doi.org/10.1016/0266-3538(91)90021-G.
4. Tiwari, S.; Bijwe, J. Surface Treatment of Carbon Fibers - A Review. *Procedia Technology* **2014**, *14*, 505-512, doi:https://doi.org/10.1016/j.protcy.2014.08.064.
5. Arnold, C.L.; Beggs, K.M.; Eyckens, D.J.; Stojcevski, F.; Servinis, L.; Henderson, L.C. Enhancing interfacial shear strength via surface grafting of carbon fibers using the Kolbe decarboxylation reaction. *Compos. Sci. Technol.* **2018**, *159*, 135-141, doi:https://doi.org/10.1016/j.compscitech.2018.02.037.
6. Beggs, K.M.; Servinis, L.; Gengenbach, T.R.; Huson, M.G.; Fox, B.L.; Henderson, L.C. A systematic study of carbon fiber surface grafting via in situ diazonium generation for improved interfacial shear strength in epoxy matrix composites. *Compos. Sci. Technol.* **2015**, *118*, 31-38, doi:https://doi.org/10.1016/j.compscitech.2015.08.001.
7. Servinis, L.; Henderson, L.C.; Andrighetto, L.M.; Huson, M.G.; Gengenbach, T.R.; Fox, B.L. A novel approach to functionalise pristine unsized carbon fiber using in situ generated

diazonium species to enhance interfacial shear strength. *J. Mater. Chem. A* **2015**, *3*, 3360-3371, doi:10.1039/C4TA04798B.

8. Pramanik, C.; Nepal, D.; Nathanson, M.; Gissinger, J.R.; Garley, A.; Berry, R.J.; Davijani, A.; Kumar, S.; Heinz, H. Molecular engineering of interphases in polymer/carbon nanotube composites to reach the limits of mechanical performance. *Compos. Sci. Technol.* **2018**, *166*, 86-94, doi:https://doi.org/10.1016/j.compscitech.2018.04.013.
9. Basova, Y.V.; Hatori, H.; Yamada, Y.; Miyashita, K. Effect of oxidation–reduction surface treatment on the electrochemical behavior of PAN-based carbon fibers. *Electrochem. Commun.* **1999**, *1*, 540-544, doi:https://doi.org/10.1016/S1388-2481(99)00112-5.
10. Pittman, C.U.; Jiang, W.; Yue, Z.R.; Gardner, S.; Wang, L.; Toghiani, H.; Leon y Leon, C.A. Surface properties of electrochemically oxidized carbon fibers. *Carbon* **1999**, *37*, 1797-1807, doi:https://doi.org/10.1016/S0008-6223(99)00048-2.
11. Pittman, C.U.; Jiang, W.; Yue, Z.R.; Leon y Leon, C.A. Surface area and pore size distribution of microporous carbon fibers prepared by electrochemical oxidation. *Carbon* **1999**, *37*, 85-96, doi:https://doi.org/10.1016/S0008-6223(98)00190-0.
12. Stojcevski, F.; Hilditch, T.B.; Gengenbach, T.R.; Henderson, L.C. Effect of carbon fiber oxidization parameters and sizing deposition levels on the fiber-matrix interfacial shear strength. *Composites, Part A* **2018**, *114*, 212-224, doi:https://doi.org/10.1016/j.compositesa.2018.08.022.
13. Gao, S.-L.; Mäder, E.; Zhandarov, S.F. Carbon fibers and composites with epoxy resins: Topography, fractography and interphases. *Carbon* **2004**, *42*, 515-529, doi:https://doi.org/10.1016/j.carbon.2003.12.085.
14. Song, W.; Gu, A.; Liang, G.; Yuan, L. Effect of the surface roughness on interfacial properties of carbon fibers reinforced epoxy resin composites. *Appl. Surf. Sci.* **2011**, *257*, 4069-4074, doi:https://doi.org/10.1016/j.apsusc.2010.11.177.
15. Jiang, J.; Yao, X.; Xu, C.; Su, Y.; Zhou, L.; Deng, C. Influence of electrochemical oxidation of carbon fiber on the mechanical properties of carbon fiber/graphene oxide/epoxy composites. *Composites, Part A* **2017**, *95*, 248-256, doi:https://doi.org/10.1016/j.compositesa.2017.02.004.
16. Park, S.-J.; Kim, B.-J. Roles of acidic functional groups of carbon fiber surfaces in enhancing interfacial adhesion behavior. *Mater. Sci. Eng. A* **2005**, *408*, 269-273, doi:https://doi.org/10.1016/j.msea.2005.08.129.
17. Park, S.-J.; Kim, M.-H. Effect of acidic anode treatment on carbon fibers for increasing fiber-matrix adhesion and its relationship to interlaminar shear strength of composites. *J. Mater. Sci.* **2000**, *35*, 1901-1905, doi:10.1023/a:1004754100310.
18. Park, S.-J.; Seo, M.-K.; Rhee, K.-Y. Studies on mechanical interfacial properties of oxy-fluorinated carbon fibers-reinforced composites. *Mater. Sci. Eng. A* **2003**, *356*, 219-226, doi:https://doi.org/10.1016/S0921-5093(03)00134-5.
19. Raghavendran, V.K.; Drzal, L.T.; Askeland, P. Effect of surface oxygen content and roughness on interfacial adhesion in carbon fiber–polycarbonate composites. *Journal of Adhesion Science and Technology* **2002**, *16*, 1283-1306, doi:10.1163/156856102320252813.
20. Rashkovan, I.A.; Korabel'nikov, Y.G. The effect of fiber surface treatment on its strength and adhesion to the matrix. *Compos. Sci. Technol.* **1997**, *57*, 1017-1022, doi:https://doi.org/10.1016/S0266-3538(96)00153-4.
21. Százdi, L.; Gulyás, J.; Pukánszky, B. Surface characterization of electrochemically oxidized carbon fibers: surface properties and interfacial adhesion. *Compos. Interf.* **2002**, *9*, 219-232, doi:10.1163/156855402760116111.
22. Eyckens, D.J.; Stojcevski, F.; Hendlmeier, A.; Arnold, C.L.; Randall, J.D.; Perus, M.D.; Servinis, L.; Gengenbach, T.R.; Demir, B.; Walsh, T.R., et al. An efficient high-throughput grafting procedure for enhancing carbon fiber-to-matrix interactions in composites. *Chem. Eng. J.* **2018**, *353*, 373-380, doi:https://doi.org/10.1016/j.cej.2018.07.133.

23. Randall, J.D.; Eyckens, D.J.; Stojcevski, F.; Francis, P.S.; Doeven, E.H.; Barlow, A.J.; Barrow, A.S.; Arnold, C.L.; Moses, J.E.; Henderson, L.C. Modification of Carbon Fiber Surfaces by Sulfur-Fluoride Exchange Click Chemistry. *ChemPhysChem* **2018**, *0*, doi:10.1002/cphc.201800789.
24. Bismarck, A.; Kumru, M.E.; Song, B.; Springer, J.; Moos, E.; Karger-Kocsis, J. Study on surface and mechanical fiber characteristics and their effect on the adhesion properties to a polycarbonate matrix tuned by anodic carbon fiber oxidation. *Composites, Part A* **1999**, *30*, 1351-1366, doi:https://doi.org/10.1016/S1359-835X(99)00048-2.
25. Mader, E.; Goa, S.-L.; Kim, J.-K. New Nano-Scale Characterization Techniques for Interphases. In *Interface Controlled Materials*, 2000; doi:10.1002/352760622X.ch38.
26. B., F.; A., A.; A., V.; F., M.; I., M. A comparative study on the influence of epoxy sizings on the mechanical performance of woven carbon fiber-epoxy composites. *Polym. Compos.* **2004**, *25*, 319-330, doi:doi:10.1002/pc.20026.
27. M., B.D.; Deepak, U.; R., K.T.; A., K.J. Evaluation of fiber surfaces treatment and sizing on the shear and transverse tensile strengths of carbon fiber-reinforced thermoset and thermoplastic matrix composites. *Polymer Composites* **1993**, *14*, 430-436, doi:doi:10.1002/pc.750140510.
28. Ma, Q.; Gu, Y.; Li, M.; Wang, S.; Zhang, Z. Effects of surface treating methods of high-strength carbon fibers on interfacial properties of epoxy resin matrix composite. *Appl. Surf. Sci.* **2016**, *379*, 199-205, doi:https://doi.org/10.1016/j.apsusc.2016.04.075.
29. Paipetis, A.; Galiotis, C. Effect of fiber sizing on the stress transfer efficiency in carbon/epoxy model composites. *Composites, Part A* **1996**, *27*, 755-767, doi:https://doi.org/10.1016/1359-835X(96)00054-1.
30. Zhang, R.L.; Huang, Y.D.; Liu, L.; Tang, Y.R.; Su, D.; Xu, L.W. Effect of emulsifier content of sizing agent on the surface of carbon fibers and interface of its composites. *Applied Surface Science* **2011**, *257*, 3519-3523, doi:https://doi.org/10.1016/j.apsusc.2010.11.066.
31. Dai, Z.; Shi, F.; Zhang, B.; Li, M.; Zhang, Z. Effect of sizing on carbon fiber surface properties and fibers/epoxy interfacial adhesion. *Appl. Surf. Sci.* **2011**, *257*, 6980-6985, doi:https://doi.org/10.1016/j.apsusc.2011.03.047.
32. Luo, Y.; Zhao, Y.; Duan, Y.; Du, S. Surface and wettability property analysis of CCF300 carbon fibers with different sizing or without sizing. *Mater. Des.* **2011**, *32*, 941-946, doi:https://doi.org/10.1016/j.matdes.2010.08.004.
33. Cheng, T.H.; Zhang, J.; Yumitori, S.; Jones, F.R.; Anderson, C.W. Sizing resin structure and interphase formation in carbon fiber composites. *Composites* **1994**, *25*, 661-670, doi:https://doi.org/10.1016/0010-4361(94)90199-6.
34. Lee, B.; Leong, K.H.; Herszberg, I. Effect of weaving on the tensile properties of carbon fiber tows and woven composites. *Journal of Reinforced Plastics and Composites* **2001**, *21*.
35. Lee, L.; Rudov-Clark, S.; Mouritz, A.P.; Bannister, M.K.; Herszberg, I. Effect of weaving damage on the tensile properties of three-dimensional woven composites. *Compos. Struct.***2002**, *57*, 405-413, doi:https://doi.org/10.1016/S0263-8223(02)00108-3.
36. Rudov-Clark, S.; Mouritz, A.P.; Lee, L.; Bannister, M.K. *Fiber damage in the manufacture of advanced three-dimensional woven composites*; 2003; Vol. 34, pp. 963-970.
37. Bijwe, J. Optimization of woven carbon fiber reinforced composites for structural and tribological applications. New Delhi, India, 2010.
38. Chou, S.; Chen, H.-C.; Chen, H.-E. Effect of weave structure on mechanical fracture behavior of three-dimensional carbon fiber fabric reinforced epoxy resin composites. *Compos. Sci. Technol.* **1992**, *45*, 23-35, doi:https://doi.org/10.1016/0266-3538(92)90119-N.
39. Neumeister, J.; Jansson, S.; Leckie, F. The effect of fiber architecture on the mechanical properties of carbon/carbon fiber composites. *Acta Mater.* **1996**, *44*, 573-585, doi:https://doi.org/10.1016/1359-6454(95)00184-0.
40. Lv, P.; Feng, Y.-y.; Zhang, P.; Chen, H.-m.; Zhao, N.; Feng, W. Increasing the interfacial strength in carbon fiber/epoxy composites by controlling the orientation and length of carbon

nanotubes grown on the fibers. *Carbon* **2011**, *49*, 4665-4673, doi:https://doi.org/10.1016/j.carbon.2011.06.064.

41. Yuan, X.; Zhu, B.; Cai, X.; Liu, J.; Qiao, K.; Yu, J. Optimization of interfacial properties of carbon fiber/epoxy composites via a modified polyacrylate emulsion sizing. *Applied Surface Science* **2017**, *401*, 414-423, doi:https://doi.org/10.1016/j.apsusc.2016.12.234.
42. Gulyás, J.; Földes, E.; Lázár, A.; Pukánszky, B. Electrochemical oxidation of carbon fibers: surface chemistry and adhesion. *Composites, Part A* **2001**, *32*, 353-360, doi:https://doi.org/10.1016/S1359-835X(00)00123-8.
43. Kainourgios, P.; Kartsonakis, I.A.; Dragatogiannis, D.A.; Koumoulos, E.P.; Goulis, P.; Charitidis, C.A. Electrochemical surface functionalization of carbon fibers for chemical affinity improvement with epoxy resins. *Appl. Surf. Sci.* **2017**, *416*, 593-604, doi:https://doi.org/10.1016/j.apsusc.2017.04.214.
44. Sharma, M.; Gao, S.; Mäder, E.; Sharma, H.; Wei, L.Y.; Bijwe, J. Carbon fiber surfaces and composite interphases. *Compos. Sci. Technol.* **2014**, *102*, 35-50, doi:https://doi.org/10.1016/j.compscitech.2014.07.005.
45. Gnädinger, F.; Middendorf, P.; Fox, B. Interfacial shear strength studies of experimental carbon fibers, novel thermosetting polyurethane and epoxy matrices and bespoke sizing agents. *Compos. Sci. Technol.* **2016**, *133*, 104-110, doi:https://doi.org/10.1016/j.compscitech.2016.07.029.
46. Stojcevski, F.; Hilditch, T.B.; Henderson, L.C. A comparison of interfacial testing methods and sensitivities to carbon fiber surface treatment conditions. *Composites, Part A* **2019**, *118*, 293-301, doi:10.1016/j.compositesa.2019.01.005.
47. Garside, M. Leading carbon fiber manufacturers by production capacity. *Statista* 2017.
48. Shono, T. Oxidation by Electrochemical Methods. In *Comprehensive Organic Synthesis*, Trost, B.M., Fleming, I., Eds. Pergamon: Oxford, 1991; https://doi.org/10.1016/B978-0-08-052349-1.00213-4pp. 789-813.
49. Elgrishi, N.; Rountree, K.J.; McCarthy, B.D.; Rountree, E.S.; Eisenhart, T.T.; Dempsey, J.L. A Practical Beginner's Guide to Cyclic Voltammetry. *J. Chem. Ed.* **2018**, *95*, 197-206, doi:10.1021/acs.jchemed.7b00361.
50. Ma, Y.J.; Wang, J.L.; Cai, X. The Effect of Electrolyte on Surface Composite and Microstructure of Carbon Fiber by Electrochemical Treatment. *Int. J. Electrochem. Sci* **2013**, *8*, 10.
51. McMican, R. Sizing stability is a key element for glass fiber manufacturing. *Reinforced Plastics* **2012**, *56*, 29-32, doi:https://doi.org/10.1016/S0034-3617(12)70110-8.
52. Dey, M.; Deitzel, J.M.; Gillespie, J.W.; Schweiger, S. Influence of sizing formulations on glass/epoxy interphase properties. *Composites, Part A* **2014**, *63*, 59-67, doi:https://doi.org/10.1016/j.compositesa.2014.04.006.
53. Kamps, J.H.; Henderson, L.C.; Scheffler, C.; van der Heijden, R.; Simon, F.; Bonizzi, T.; Verghese, N. Electrolytic Surface Treatment for Improved Adhesion between Carbon Fiber and Polycarbonate. *Materials* **2018**, *11*, 2253, doi:10.3390/ma11112253.
54. Nexus, C. https://www.carbonnexus.com.au/. Availabe online: (accessed on 3/07/2019).
55. Feih, S.; Wonsyld, K.; Minzari, D.; Westermann, P.; Lilholt, H. *Testing Procedure for the Single Fiber Fragmentation Test*; Forskningscenter Risø: 2004.
56. Buckley, J.D.; Edie, D.D. *Carbon-Carbon Materials and Composites*; Noyes Publications: New Jersey, USA, 1993.
57. Kim, J.-K.; Mai, Y.-w. High strength, high fracture toughness fiber composites with interface control—A review. *Compos. Sci. Technol.* **1991**, *41*, 333-378, doi:https://doi.org/10.1016/0266-3538(91)90072-W.
58. Johnson, J.W.; Thorne, D.J. Effect of internal polymer flaws on strength of carbon fibers prepared from an acrylic precursor. *Carbon* **1969**, *7*, 659-661, doi:https://doi.org/10.1016/0008-6223(69)90520-X.

59. Brocks, T.; Cioffi, M.O.H.; Voorwald, H.J.C. Effect of fiber surface on flexural strength in carbon fabric reinforced epoxy composites. *Appl. Surf. Sci.* **2013**, *274*, 210-216, doi:https://doi.org/10.1016/j.apsusc.2013.03.018.
60. Fukunaga, A.; Ueda, S. Anodic surface oxidation for pitch-based carbon fibers and the interfacial bond strengths in epoxy matrices. *Compos. Sci. Technol.* **2000**, *60*, 249-254, doi:https://doi.org/10.1016/S0266-3538(99)00118-9.
61. Xu, Z.; Chen, L.; Huang, Y.; Li, J.; Wu, X.; Li, X.; Jiao, Y. Wettability of carbon fibers modified by acrylic acid and interface properties of carbon fiber/epoxy. *European Polymer Journal* **2008**, *44*, 494-503, doi:https://doi.org/10.1016/j.eurpolymj.2007.11.021.
62. Jesson, D.A.; Watts, J.F. The Interface and Interphase in Polymer Matrix Composites: Effect on Mechanical Properties and Methods for Identification. *Polym. Rev.* **2012**, *52*, 321-354, doi:10.1080/15583724.2012.710288.
63. Nakao, F.; Takenaka, Y.; Asai, H. Surface characterization of carbon fibers and interfacial properties of carbon fiber composites. *Composites* **1992**, *23*, 365-372, doi:https://doi.org/10.1016/0010-4361(92)90336-S.
64. Hendlmeier, A.; Marinovic, L. I.; Al-Assafi, S.; Stojcevski, F.; Henderson, L. C. Sizing effects on the interfacial shear strength of a carbon fibre reinforced two-component thermoplastic polymer. *Composites, Part A.* **2019**, *127*, 105622-105630, doi: https://doi.org/10.1016/j.compositesa.2019.105622

The authors declare no conflict of interest.